Efficient Double Helix Detection with Steerable Filters

Andrew E. S. Barentine [1,*,✉], Ashwin Balaji[1,2,*] and W.E. Moerner [1]

[1]Department of Chemistry, Stanford University, Stanford, California 94305, USA

[2]Biophysics PhD Program, Stanford University, Stanford, California 94305, USA

[*]these authors contributed equally

✉ andrewesbarentine@gmail.com

August 15, 2025

Abstract

We present an efficient detection scheme for localization of Double Helix point-spread functions for 3D single-molecule localization microscopy or tracking. Using steerable filters, we extract both 2D position and lobe orientation (axial position) estimates using just 7 convolutions, orders of magnitude less than used in deep learning based approaches. For a complete SMLM analysis pipeline, we pair this detection with a fitter using an optimally parameterized double Gaussian model, and implement both as a plugin for the open source PYthon Microscopy Environment (PYME).

Point-spread functions (PSFs) engineered to encode additional information for single-molecule localization microscopy (SMLM) can become considerably more difficult or computationally inefficient to detect and localize. Open-aperture PSFs can be readily detected on a camera frame using a matched difference of Gaussians filter, which requires just 2 (separable) convolutions of the camera frame. However, engineered PSFs can produce far more complex spatial patterns that may or may not change significantly with defocus. The requirement to detect emitters on many (10^4 - 10^7) camera frames makes computational speed an imperative, and the accuracy of initial parameter estimates can additionally improve the performance of localization fitting.

The Double Helix (DH) is an engineered PSF with two lobes which rotate with defocus, and as such is typically used to encode axial position of emitters in the orientation of the two lobes of the imaged PSFs [1] as shown in Figure 1A. The DH PSF is often modeled using a double Gaussian function,

$$gg\left(x,y\right) = A_1 e^{-\frac{\left(x-x_1\right)^2+\left(y-y_1\right)^2}{2\sigma^2}} + A_2 e^{-\frac{\left(x-x_2\right)^2+\left(y-y_2\right)^2}{2\sigma^2}}, \tag{1}$$

where A_i, x_i, and y_i are the amplitudes and center positions of each Gaussian, and σ is the shared width parameter. For the DH PSF, we find it more natural to perform a change of variables such that the center position of the PSF, (x_O, y_O), the separation between its lobes, L, and lobe orientation, θ, (see Fig. 1B) can be directly fitted:

$$gg\left(x,y\right) = A_1 e^{-\frac{\left(x-x_\mathrm{O}-0.5L\cos\theta\right)^2+\left(y-y_\mathrm{O}-0.5L\sin\theta\right)^2}{2\sigma^2}} + A_2 e^{-\frac{\left(x-x_\mathrm{O}+0.5L\cos\theta\right)^2+\left(y-y_\mathrm{O}+0.5L\sin\theta\right)^2}{2\sigma^2}}. \tag{2}$$

With defocus across the designed axial range, θ rotates roughly π rad, yet the overall double-lobed structure of the DH PSF remains consistent, with minimal changes to L and σ (see figure 1B,C). In addition to efficient detection of candidate molecules for fitting, the ideal detection algorithm would provide accurate estimates for the position and orientation of each candidate (x_o, y_o), and θ.

The classic method of detection implements a series of matched filters at a number of orientations on each frame of the SMLM acquisition [2]. Using a finite number of these candidate filters leads to some orientations being more efficiently detected than others and errors in initial orientation estimates, which can become computationally expensive to avoid by increasing the number of oriented filters used. Deep-learning approaches to DH PSF detection often use even more convolutions, typically in the range of hundreds to thousands. Here, we use a steerable filter design and an edge orientation algorithm developed by Freeman and Adelson [3] to detect DH PSFs and analytically estimate their orientation with just 7 (separable) convolutions.

Optimal steerable filters have been developed for several SMLM use cases [4], including DH PSF detection [5]. Here, we instead implemented the 2nd derivative of a two-dimensional Gaussian filter (G_2) because it has a low number of basis filters (7) and there exists an analytic expression for the orientation that maximizes the response at each pixel as previously derived [3]. The $G_2^{\theta=0}$ filter is given by

$$G_2^{\theta=0}(x, y) = \frac{(x - \sigma_f)(\sigma_f + x)e^{-\frac{x^2+y^2}{2\sigma_f^2}}}{2\pi\sigma_f^4}, \tag{3}$$

where σ_f is the filter width parameter. $gg(y = 0)$, $G_2^{\theta=0}(y = 0)$, and their squared convolution are shown in Figure 1E. Despite the discrepancy between the filter and the model, the squared filter output still peaks at the center of the model as desired, provided σ_f is chosen within a reasonable range.

After convolving a raw camera frame with just 3 oriented G_2^{θ} filters, a linear combination of these 3 convolutions can be used to construct the frame convolved with any orientation of the G_2 filter without performing the final desired convolution explicitly [3]. Further, there exists a set of separable basis kernels (as shown in figure 1F). The Hilbert transform of G_2, H_2, can be reasonably approximated with a 3rd-order polynomial, and requires 4 basis filters to steer [3]. These Hilbert transformed filters (Fig. 1F) share the same spatial frequency response, but with a phase shift from the G_2 filtering [7]. Freeman and Adelson show that adding the G_2 and H_2 filtered outputs in quadrature can be approximated by a truncated Fourier expansion from which the strength of the response and the angle maximizing it can be calculated [3], resulting in filtered strength (Fig. 1G) and orientation maps (Fig. 1H) of the input image.

We use per-pixel signal-to-noise (SNR) based thresholding to detect candidates across a large dynamic range of brightness with minimal user input [8]. The noise-based threshold map is squared such that it can be applied to the strength map. The strength map and threshold map are each maximum filtered in order to extract the position in the strength map (which peaks at the center of the DH PSF) corresponding to the molecular position of the imaged DH PSF lobes above the SNR threshold. A precise orientation estimate for each candidate is then indexed out of the orientation map (Fig. 1H). In short, high-quality DH PSF detections and orientation estimates are extracted from each SMLM frame with just 7 convolutions and 2 maximum filters (see figure 1I).

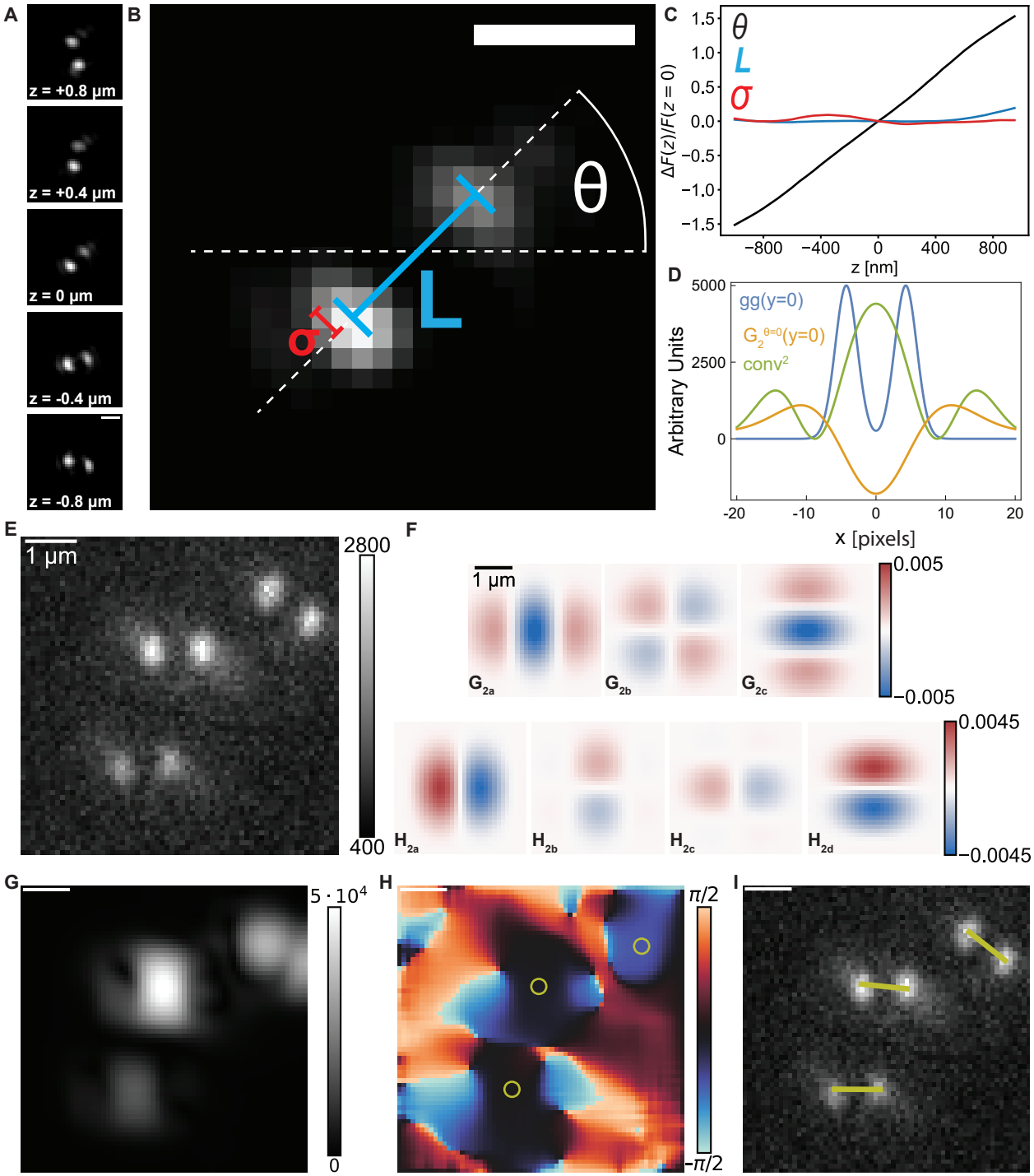

Figure 1: A) An experimental DH PSF z-stack. B) The z = 0 nm slice from (A), showing the lobe width parameter σ, the lobe separation parameter L, and the orientation parameter θ for the double Gaussian model of eq. 2. C) Fitted calibration curves for θ, L, and σ, all shown as fractional changes relative to their z = 0 values. D) 1D squared convolution of the double Gaussian model $gg\,(y = 0)$, with parameters $A_1 = A_2 = 5000$ and $L = 8.54, \sigma = 1.58, \sigma_f = 6.25$ [pixels]. $G_2^{\theta=0}\,(y = 0)$ is plotted on its own scale. E) A simulated DH PSF SMLM frame from [6]. F) The separable G_2 and H_2 basis filter kernels for $L = 10.25, \sigma = 2.15, \sigma_f = 5.5$ [pixels]. G) The strength map resulting from filtering (E). H) The orientation map resulting from filtering (E). Yellow circles highlight detected emitter positions. I) Detected emitter positions and orientations drawn as yellow sticks overlaid on (E). All scale bars are 1 µm.

Discussion

We deployed this detection and accompanying double Gaussian fit as a plugin for the PYthon Microsocpy Environment (PYME) in order to leverage its SNR-based thresholding, percentile-based background estimation, and performant (distributed) analysis capabilities [9, 10]. Our plugin includes calibration routines to determine the optimal filter parameter σ_f from a DH PSF calibration z-stack and a module for converting fitted orientation to axial emitter position. Fitting a model in which θ appears directly (eq. 2) facilitates facile uncertainty estimation on θ and therefore z position. Uncertainty estimates for θ, L, σ, and other parameters are readily available for filtering localizations in PYMEVisualize [11], as are lobe amplitude asymmetry ($\min\left[A_i\right] / \max\left[A_i\right]$), and deviation from expected L or σ for a given z position. Finally, we find filtering on the deviation of fitted center position from the initial detected position to aid in removing spurious detections on the edges of especially bright emitters (e.g. fiducial beads) that exhibit fringes to the outside of each lobe.

We hope this software is immediately useful to users of DH PSFs. Additional effort to accelerate the described detection and fitting could yield particularly fast 3D position estimates suitable for real-time drift correction or repositioning in tracking experiments. Similar orientation estimation from steerable filters might also be developed for filter sets which are more optimally matched to DH or other engineered PSFs.

Funding

This work was supported in part by the National Institute of General Medical Sciences Grant No. R35GM118067.

Acknowledgment

We are especially grateful to David Baddeley for developing and maintaining PYME.

Disclosures

W.E.M. is a member of the Scientific Advisory Board for Double-Helix Optics.

Data availability

The described software is available at reference [12]. The simulated DH PSF SMLM data is frame 7062 of the MT0.N1.LD-DH dataset from reference [6] and is available for download from srm.epfl.ch/Challenge/ChallengeSimulatedData.

References

1. Pavani, S. R. P. & Piestun, R. Three dimensional tracking of fluorescent microparticles using a photon-limited double-helix response system. *Opt. Express* **16,** 22048–22057. doi:10.1364/OE.16.022048 (2008).
2. Bayas, C., von Diezmann, A., Gustavsson, A.-K. & Moerner, W. E. Easy-DHPSF 2.0: open-source software for three-dimensional localization and two-color registration of single molecules with nanoscale accuracy V.2. *Prot. Exch.* doi:10.21203/rs.2.9151/v2 (2019).
3. Freeman, W. & Adelson, E. The design and use of steerable filters. *IEEE Transactions on Pattern Analysis and Machine Intelligence* **13,** 891–906. doi:10.1109/34.93808 (1991).
4. Aguet, F., Geissbühler, S., Märki, I., Lasser, T. & Unser, M. Super-resolution orientation estimation and localization of fluorescent dipoles using 3-D steerable filters. EN. *Optics Express* **17,** 6829–6848. doi:10.1364/OE.17.006829 (2009).

5. Fageot, J. *et al.* Principled Design and Implementation of Steerable Detectors. *IEEE Transactions on Image Processing* **30,** 4465–4478. doi:10.1109/TIP.2021.3072499 (2021).

6. Sage, D. *et al.* Super-Resolution Fight Club: Assessment of 2D and 3D Single-Molecule Localization Microscopy Software. *Nature Methods* **16,** 387–395. doi:10.1038/s41592-019-0364-4 (2019).

7. Bracewell, R. N. *The Fourier transform and its applications* 3rd ed. en (McGraw Hill, Boston, 2000).

8. Lin, R., Clowsley, A. H., Jayasinghe, I. D., Baddeley, D. & Soeller, C. Algorithmic corrections for localization microscopy with sCMOS cameras - characterisation of a computationally efficient localization approach. EN. *Optics Express* **25,** 11701–11716. doi:10.1364/OE.25.011701 (2017).

9. Baddeley, D. *et al. python-microscopy* version 25.03.27. 2025. doi:10.5281/zenodo.8042213.

10. Barentine, A. E. S. *et al.* An integrated platform for high-throughput nanoscopy. *Nature Biotechnology* **41,** 1549–1556. doi:10.1038/s41587-023-01702-1 (2023).

11. Marin, Z. *et al.* PYMEVisualize: an open-source tool for exploring 3D super-resolution data. en. *Nature Methods* **18,** 582–584. doi:10.1038/s41592-021-01165-9 (2021).

12. Barentine, A. E. S. & Balaji, A. *barentine/double_helix: 25.08.14* version 25.08.14. 2025. doi:10.5281/zenodo.16877693.